Synthesis of new lamellar inorganic–organic talc-like hybrids

Jean-Christophe Gallégo, Maguy Jaber,* Jocelyne Miehé-Brendlé and Claire Marichal

Received (in Montpellier, France) 24th August 2007, Accepted 8th October 2007
First published as an Advance Article on the web 8th November 2007
DOI: 10.1039/b713004j

One-step sol–gel syntheses of lamellar organic–inorganic hybrids with a talc like structure are performed using *N*-phenylaminomethyltrimethoxysilane (PAM-TMS) and phenethyltrimethoxysilane (PE-TMS) as silicon sources. Results obtained by X-ray diffraction and X-ray fluorescence show that after one day of ageing at room temperature, talc-like hybrids (TLH) are obtained. The FTIR spectra drive to the conclusion that the organic moieties are present in the structure. The integrity of these was confirmed by ^{13}C solid-state CP MAS NMR. ^{1}H–^{13}C CP MAS NMR magnetization curves performed on both samples seem to indicate a lower mobility for the phenylaminomethyl pending group. ^{29}Si MAS NMR spectra show a majority of highly condensed silicon environments for PE-TLH whereas a significant amount of low condensed species are detected for PAM-TLH. TEM micrographs reveal exfoliated layers for phenethyl based materials.

Introduction

The possibility to combine properties of organic and inorganic components for materials design and processing is a very old challenge that likely started since ages (Egyptian inks, green bodies of china ceramics, prehistoric frescos, ...).

Organic–inorganic hybrids do not represent only a creative alternative to design new materials but their improved or unusual features allow the development of innovative industrial applications.[1]

Concerning the inorganic framework, clays and especially smectite are of particular interest, owing to their adsorption properties, thermal stability and swellability in polar solvents. They are made of stacking of layers composed by one octahedral sheet (O) occupied by an hexacoordinated element such as Mg sandwiched between two tetrahedral (T) silicic sheets in the well known talc structure as shown in Fig. 1.

The term organic–inorganic clay hybrid gathers intercalated and functionalized clays. Indeed, the intercalation of quaternary ammonium ions between the layers by cationic exchange owing to the charge of the structure was reported by Williams-Daryn and Thomas.[2] Organoclays can also be obtained by a post-synthesis treatment in the presence of an organo-alkoxysilane as realized by Carrado *et al.*[3] However a new route for clay hybrid synthesis was proposed since 1995 by Fukushima and Tani.[4] Functionalization of clays can be achieved by a one-step synthesis leading to new materials with organic moieties *covalently* linked to the silicon atoms of the tetrahedral sheets and pending in the interlayer space. This sol–gel synthesis of a talc-like hybrid (TLH) with the following chemical formula: $Mg_3(RSi)_4O_8(OH)_2$ is performed at room temperature for 24 h using organotrialkoxysilane ($RSi(OR')_3$), as a silicon source, where R stands for the organic part and R′ for ethoxy or methoxy groups. The nature of the organic groups in the interlayer space allows the tailoring of the properties of the TLH. Linear alkyl[5–7] and functionalized linear alkyl[8–10] as well as phenyl[5,11] have been used for the synthesis of this type of hybrids. More precisely 3-aminopropyl and 3-mercaptotrialkoxysilane were widely used for the adsorption properties of the resultant hybrids.[12–19] Catalytic, electroanalysis and heavy-metals retention applications were reported in the literature.[10] The role of the length of the organic moiety in these syntheses of clay-like hybrids was demonstrated by Ukrainczyk *et al.* in 1997.[5] One of the conclusions of these authors was the increasing of the ordering degree of these materials by increasing the length of the organic moieties. Furthermore, the synthesis of phenyl talc-like hybrids was also described in this article and a high condensation state of the silicic species was obtained. Consequently, combining the two functions (linear alkyl chain and a phenyl group) is expected to lead to well organized hybrid materials that can be used as precursors for the preparation of clay-polymers nanocomposites.

This is the reason why organosilanes of the type phenethyl ($C_6H_5CH_2CH_2$–) and phenylaminomethyl ($C_6H_5NHCH_2$–)

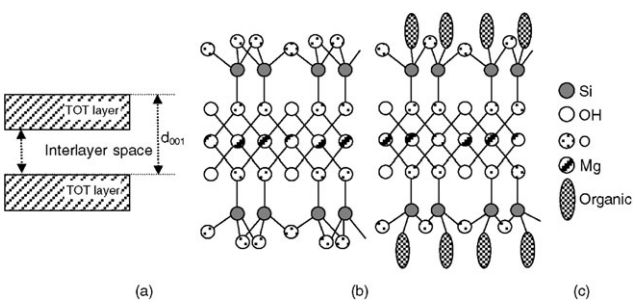

Fig. 1 (a) Representation of the clay structure. (b) TOT layer structure of a natural talc. (c) Proposed TOT layer structure of an organic–inorganic talc-like hybrid.

Laboratoire de Matériaux à Porosité Contrôlée, UMR CNRS 7016, Ecole Nationale Supérieure de Chimie de Mulhouse, Université de Haute-Alsace, 3 rue Alfred Werner, F-68093 Mulhouse Cedex, France. Fax: +33 (0)389336885; Tel: +33 (0)389336708. E-mail: maguy.jaber@uha.fr

were chosen for talc-like hybrid preparation by one-step sol–gel synthesis. The organization of the lattice and the degree of crystallinity of these new materials are evaluated by different technics such as XRD, FTIR, TEM, XRF, TG-DTA and solid-state NMR.

Experimental

Reactants

N-Phenylaminomethyltrimethoxysilane $PhNHCH_2Si(OCH_3)_3$ (Wacker, Geniosil XL 973, >95 wt%), phenethyltrimethoxysilane $Ph(CH_2)_2Si(OCH_3)_3$ (ABCR, >97 wt%), magnesium nitrate hexahydrate $Mg(NO_3)_2{\cdot}6H_2O$ (Fluka, ≥ 99 wt%), ethanol CH_3CH_2OH (Riedel-de Haën, 99.8 wt%), sodium hydroxide NaOH (Fluka, ≥ 99%) and distilled water were used without further purification.

Synthesis

Phenylaminomethyl- and phenethyl-talc like hybrid materials (PAM-TLH and PE-TLH, respectively) were prepared by mixing the organotrialkoxysilane with an ethanolic solution of magnesium nitrate with a Si/Mg molar ratio equal to 1.33. The initial molar composition is: $1\,RSiO_{3/2} : 0.167\,MgO : 0.167\,NaO : 107\,EtOH : 185\,H_2O$. In both cases 1.2×10^{-2} mol of the organosilane were added under stirring to 75 cm^3 of a fresh magnesium nitrate ethanolic solution (0.12 mol dm^{-3}). The gel was precipitated under stirring by the slow addition of 40 cm^3 of an aqueous solution of sodium hydroxide (0.5 mol dm^{-3}) until a pH of 11 was obtained. Afterwards the mixture was aged without stirring for 24 h at room temperature resulting in PAM-TLH and PE-TLH materials. Finally, the gel was centrifuged and the recovered solid washed three times with 200 cm^3 of distilled water and dried at 80 °C under air during 24 h.

Characterization

X-Ray diffraction (XRD) patterns of the hybrid materials were recorded using a Philips X-pert diffractometer operating with Cu-Kα radiation (λ = 0.15418 nm), between 3 and 70° 2θ with a step size of 0.02° per 2s.

Fourier transform infrared (FTIR) measurements were performed in the region of 400–5000 cm^{-1} using a Bruker Equinox 55 spectrometer with a DTGS detector and analyzed with OPUS software. The number of scans was fixed to 100 and the resolution was 2 cm^{-1}. KBr pellets of the materials were prepared using IR-grade potassium bromide.

The thermogravimetric analysis of the as-synthesized samples were realized with a TG-DTA apparatus (Setaram Labsys) under air and argon, with a flow rate of about 1.5 $dm^3\,h^{-1}$ from 25 to 1000 °C and a heating rate of 5 °C min^{-1}. A reference experiment was recorded to correct base line deviation.

Elemental analyses of Si, Mg and Na were performed by X-ray fluorescence (XRF) with a Magix Philips (2.4 kW). The samples were packed into pellets. Prior to analysis, calibration was performed with mixtures of SiO_2 and $MgCl_2$ at different concentrations. C and N contents were determined by combustion at 1050 °C followed by IR detection (C) or gas catharometry (N) at the "Service central d'analyse du CNRS at Solaize".

^1H decoupled ^{29}Si magic angle spinning (MAS) NMR and ^1H–^{13}C cross polarization magic angle spinning (CP MAS) NMR spectra were recorded on a Bruker DSX-400 spectrometer (B_0 = 9.4 T) operating at 79.460 and 100.577 MHz, respectively. Samples were packed in either a 7 mm (^{29}Si) or a 4 mm (^{13}C) diameter cylindrical zirconia rotor and spun at a spinning frequency of 4 and 14.5 kHz, respectively. For ^{29}Si MAS NMR a π/4 pulse duration of 1.7 μs with a recycle delay of 60 s were used. Variable contact time ^1H–^{13}C CP MAS experiments were performed in order to probe the mobility of the organic moieties in the interlayer space. These experiments were recorded with a proton π/2 pulse duration of 5 μs, a contact time between 6 μs and 10 ms and a recycle delay of 8 s. Deconvolution of the NMR spectra were performed with the dmfit software[20] which gives the relative proportion of each component.

Transmission electron microscopy (TEM) investigations were carried out on a Philips CM 200 microscope operating at 200 kV. Prior to observation, the powders were ground and mixed with either a polymer matrix (SpeciFix resin and SpeciFix-20 curing agent from Struers) based on Bisphenol A ($HOC_6H_4CMe_2C_6H_4OH$) or dispersed in ethanol. For the resin, the mixture was cured during 3 d on the top of a drying oven before analysis. An LKB 8800 Ultrotone III was used to obtain 50–100 nm thick slices. For ethanol dispersions, one droplet was deposited onto a carbon-coated copper grid and left to dry in air, prior to analysis.

Results and discussion

Fig. 2 shows the X-ray diffraction patterns of the as-synthesized PAM-TLH and PE-TLH materials. Four main diffraction reflections occurring at 5, 18, 35 and 59° 2θ are observed. These peaks are broader than those of the parent talc material

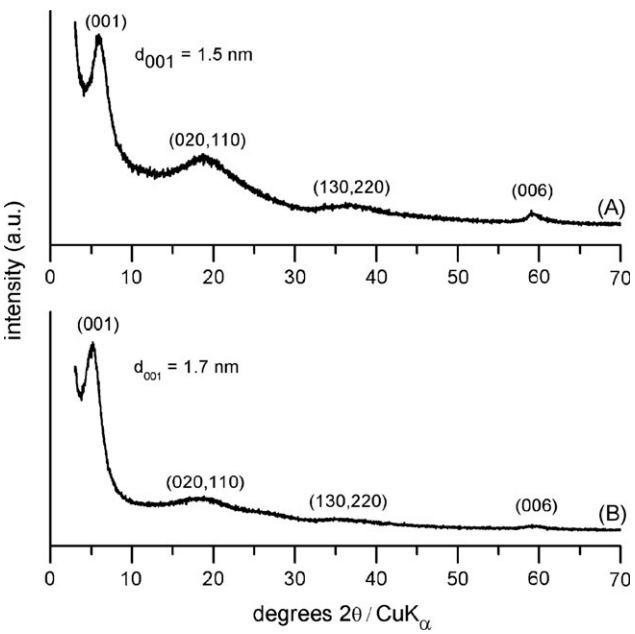

Fig. 2 XRD patterns of PE-TLH (A) and PAM-TLH (B).

indicating a lower organization of the structure due to the presence of organic chains.[21] According to general indexation of organic–inorganic talc like hybrids diffraction patterns, these peaks correspond to (001), (020, 110), (130, 220) and (060) reflections.[5,22] The d_{001} periodicity is the sum of the interlayer distance and the layer thickness (0.96 nm in the case of the parent talc).[23] The experimental d_{001} periodicities are 1.7 nm for PAM-TLH and 1.5 nm for PE-TLH (Fig. 2). An interlayer distance of 0.7 and 0.5 nm can thus be deduced for PAM-TLH and PE-TLH, respectively. The maximum length of the PAM and PE organic pendant groups is about 0.8 nm estimated from ACD/ChemSketch 9.04 software. This value is close to the interlayer distance estimated for the PAM-TLH material suggesting an alternated monolayer of pending PAM groups. On the contrary, the distance of 0.5 nm measured for the PE-TLH material is too small to accommodate such a packing. In this latter material, the PE organic chains are most probably bent. The (060) reflection observed at 59° 2θ (0.156 nm) is characteristic of the trioctahedral character as generally observed in talc.[6,21]

The lamellar structure of the different solids has been revealed by XRD. Since the organization at long distance was generally weak for this type of materials TEM experiments were performed. PE-TLH (Fig. 3) micrographs show well exfoliated 25 nm long clay layers. A micrograph of the PAM-TLH material (Fig. 4) exhibits well stacked layers with a 85 nm length. Exfoliation of PE-TLH samples is probably explained by the shorter layer length. Indeed, fewer interactions between organic moities per layer occur in shorter layers. Consequently exfoliation could be favored whatever the dispersion method (resin or solvent) for TEM observation.

The composition of the hybrid materials was determined by chemical analysis and results are reported in Table 1. Molar Si/Mg ratios obtained are close to the theoretical value (1.33) for both materials. Small amounts of Na are also present in the interlayer space. The values of C/Si and C/N ratios (Table 1) are in agreement with the expected values indicating that the organic moieties are not modified during the hybrid synthesis.

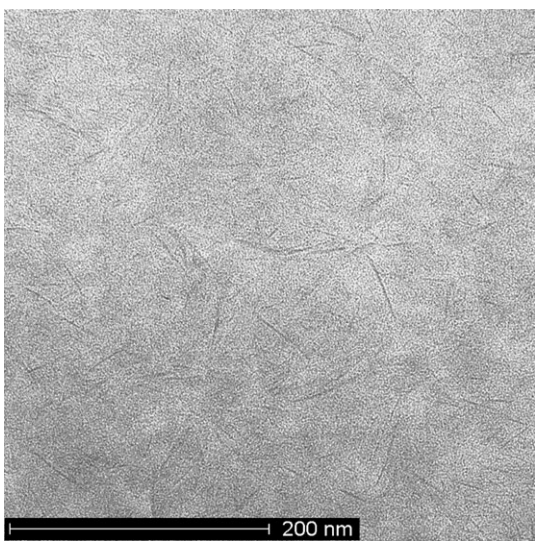

Fig. 3 TEM micrograph of PE-TLH.

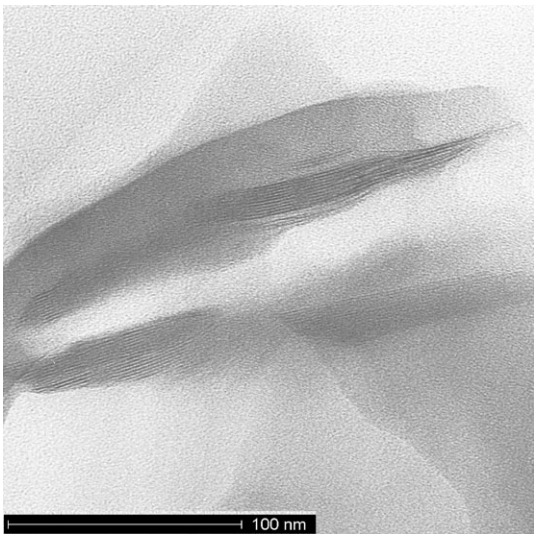

Fig. 4 TEM micrograph of PAM-TLH.

The thermal behaviour of these organoclay materials was investigated by TG/DTA thermal analysis. DTA curves of the PAM-TLH (Fig. 5) material display two exothermic peaks at 250 and 450 °C corresponding to the oxidation of the organic moieties. An endothermic peak at 75 °C is assigned to physisorbed water.

The exothermic peak at 850 °C corresponds to the reorganisation of the inorganic framework into an enstatite ($MgSiO_3$) structure as proven by XRD (not shown). To confirm the assignment of the different peaks TG/DTA analysis has been realized under argon atmosphere (not shown). The peaks at 70–75 and 850 °C are unchanged confirming the suggested attribution. The shape of TG/DTA curves for PE-TLH is similar those of PAM-TLH. Nevertheless the oxidation of the organic moieties occurs at 370 and 500 °C. Water loss and recrystallization are observed at 70 and 850 °C, respectively. Organic contents obtained by TG/DTA were compared to the theoretical values expected from the ideal formula: $Mg_3(RSi)_4O_8(OH)_2$ (Table 2). A good agreement between theoretical and experimental values is observed for both hybrids.

Structural bonds have been identified by FTIR for both materials (Fig. 6). The aromatic C–H bonds are represented in PE-TLH spectra by δ_{CH} bands at 703 and 744 cm^{-1}, and ν_{CH} bands at 1758, 1804, 1872, 1944, 3026, 3062, 3085 cm^{-1}. The C–C bonds of the rings give peaks at 1603, 1454 and 1410 cm^{-1}. Finally the bands at 1056, 3202, 830, 3701 cm^{-1} are attributed to ν_{SiOSi}, $\nu_{OH\ (Si)}$, $\delta_{OH\ (Si)}$ and ν_{Mg-OH}, respectively. Significant differences are observed between PE-TLH and PAM-TLH FTIR spectra as shown by the weakest intensity of the bands corresponding to C–C and C–H aromatic bonds. The observation of vibration bands at 1511 (δ_{CHN}), 1318 (ν_{CN}) and 1178 cm^{-1} (ν_{NR}) confirmed the presence of the amino-substituted ring.

^{1}H–^{13}C CP MAS NMR was also used to check the integrity of the organic pendant groups. The spectra of PAM-TLH and PE-TLH (Fig. 7) show the typical resonances of the *N*-phenylaminomethyl and phenethyl organic moieties, respectively. The assignment of each resonance, thanks to the ACD/

Table 1 Experimental Si to Mg molar ratio and Na content of the different samples deduced from chemical analysis

Sample	Si/Mg molar ratio	C/Si molar ratio	C/N molar ratio	Na (wt%)
PAM-TLH	1.20 ± 0.07	6.68 ± 0.06	7.0 ± 0.45	0.409
PE-TLH	1.15 ± 0.07	8.44 ± 0.11	—	0.636

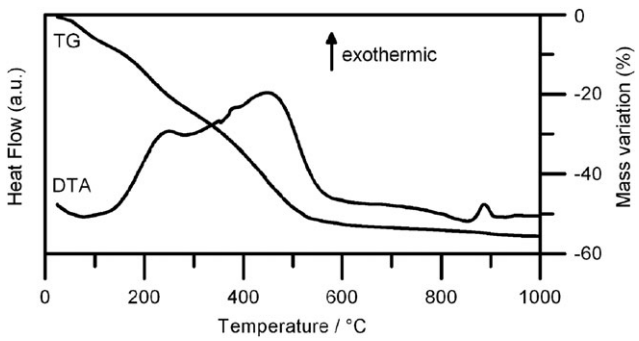

Fig. 5 Weight loss and heat flow curves for the PAM-TLH material.

ChemSketch 9.04 software, is reported on the corresponding spectra according to the atom numbering of the organic group given in the inset of Fig. 7. The resonances between 120 and 150 ppm correspond to the phenyl ring whereas the CH_2 groups are detected between 15 and 32 ppm indicating that the organic moieties are intact. The absence of a resonance at 50 ppm corresponding to methoxy groups confirms the total hydrolysis of methyl groups for PAM-TLH and PE-TLH.

^{1}H–^{13}C CP MAS NMR also inform about the molecular motion of the organic groups. Indeed, during CP from ^{1}H to ^{13}C, the ^{13}C magnetization (I) increases according to eqn (1) with the time constants T_{CH} that probe the mobility of the corresponding carbon. A shorter T_{CH} corresponds to faster CP rate indicating a less mobile carbon group since motion averages the ^{1}H–^{13}C dipolar interaction decreasing the CP efficiency. CP time constants T_{CH} are derived from variable contact time experiments given in Fig. 7 for the resolved resonances corresponding to carbon 1 of the phenyl groups and 8 (CH_2) of PAM-TLH and PE-TLH. The calculated values of T_{CH} are detailed in Table 3. The other resonances accounting for several carbons are of less use in this regard. The good agreement between experimental data and the curve calculated according to eqn (1) is of note. The highest T_{CH} values (0.42 ms; 0.25 ms) are obtained for carbon 1 of the phenyl groups, as expected for a quaternary carbon; T_{CH} values for CH_2–Si groups (carbon 8) are significantly lower (0.046 and 0.030 ms for PE-TLH and PAM-TLH, respectively). The values are close to what is usually found for CH_2 groups of surfactants in intercalated clay minerals.[23] Interestingly, whatever the carbon, T_{CH} values are greater for PE-TLH than for PAM-TLH that could indicate a lower mobility for the organic moieties in the former material. This is probably caused by the electronic delocalization including the nitrogen atom in the PAM ring. Computing calculations are underway in order to support this hypothesis.

Table 2 Experimental and theoretical organic content of the different samples determined by TG

Sample	Found (%)	Calc. (%)
PAM-TLH	51	55
PE-TLH	53	55

^{1}H decoupled ^{29}Si MAS NMR allows to study the environment of silicon atoms in the clay framework, and by extension, the degree of polycondensation of the structure. The T^n notation which is commonly used in the literature corresponds to the number of OM (M = Si or Mg) connections that a silicon has: $Si(R)(OM)_n(OH)_{3-n}$, R being the organic moiety (PAM or PE).[24]

The ^{29}Si MAS NMR spectra of the PAM-TLH [Fig. 8(A)] material present a broad asymmetric resonance in a range of chemical shift values between −65 and −40 ppm indicating that the PAM groups are covalently bonded to the inorganic layers. Despite the low resolution of the spectrum, deconvolution into three components at −70, −57 and −50 ppm, respectively assigned to T^3, T^2 and T^1 can be suggested. The corresponding proportions of each species are reported in Table 4. It is interesting to note the low ratio of T^3 units for PAM-TLH materials indicating that the tetrahedral layers are weakly condensed. This result could be explained by geometric constraints due to the low mobility of the phenyl ring of the organic moiety as shown by ^{13}C NMR.

The ^{29}Si MAS NMR spectrum of the PE-TLH material shown in Fig. 8(B) is different from that of the PAM-TLH material. Indeed, three well resolved resonances are observed at −68, −58 and −50 ppm corresponding, respectively to T^3, T^2 and T^1 units with the proportions being given in Table 4. In contrast to the PAM-TLH sample, the PE-TLH material presents 74% of T^3 sites indicating a well condensed inorganic framework. These values are in agreement with the 78% value

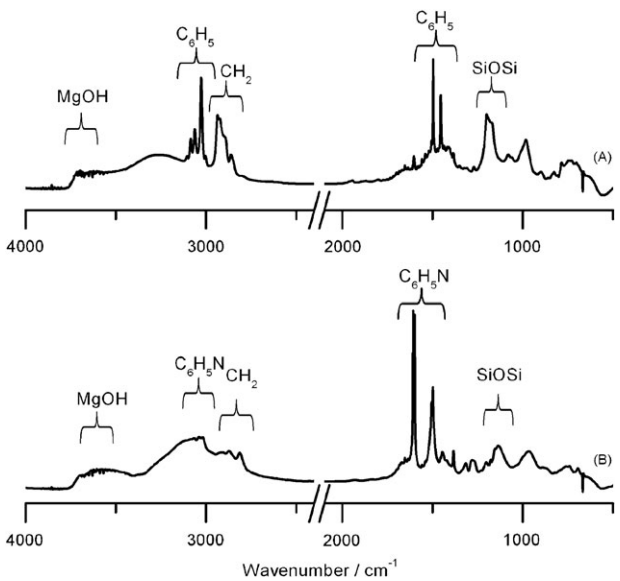

Fig. 6 FTIR spectra of PE-TLH (A) and PAM-TLH (B).

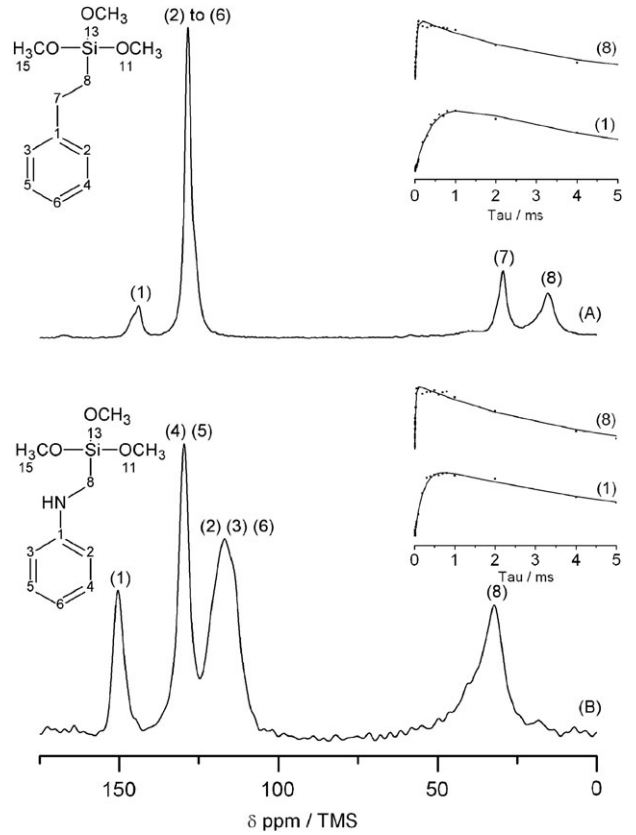

Fig. 7 ^{1}H–^{13}C CP MAS NMR spectra of PE-TLH (A) and PAM-TLH (B) materials at a spinning frequency of 14.5 kHz. The contact time *vs.* peak intensity curves for the common resolved resonances are shown in the insets.

observed for Phenyl-TLH in the literature.[5,18] It is also of note that no resonance appears in range −90 to −102 ppm indicating the absence of silicon which is not bonded to an organic chain.

The presence of T^1 and T^2 species indicates that some silicon atoms of the tetrahedral sheets are not completely bonded to the brucite layer or to another silicon and present silanol functions. One part of the chemical formula can be deduced from the ^{29}Si NMR data. Indeed, the knowledge of the proportions of T^1 and T^2 sites allows to determine the number

Table 3 Data from the variable contact time ^{1}H–^{13}C CP MAS NMR experiments for PE-TLH and PAM-TLH materials calculated according to eqn (1)[a]

PE-TLH			PAM-TLH		
δ/ppm	$T_{1\rho H}$/ms	T_{CH}/ms	δ/ppm	$T_{1\rho H}$/ms	T_{CH}/ms
144	5.3 ± 0.3	0.42 ± 0.02	150	14 ± 5	0.25 ± 0.08
15	3.7 ± 0.3	0.046 ± 0.002	32	6.0 ± 0.7	0.030 ±0.004

$$I = \frac{I_0}{1-(k_1/k_2)}[\exp(-k_1 t) - \exp(-k_2 t)] \quad (1)$$

[a] Cross-polarization equation for peak intensity/contact time fitting.[25] I/I_0 is the cross-polarization efficiency, I_0 is the intensity under conditions of full cross-polarization and no relaxation, I is the peak intensity, t is the contact time, k_1 is the relaxation rate in rotating frame (= $1/T_{1\rho H}$) and k_2 is the rate of cross-polarization ($1/T_{CH}$).

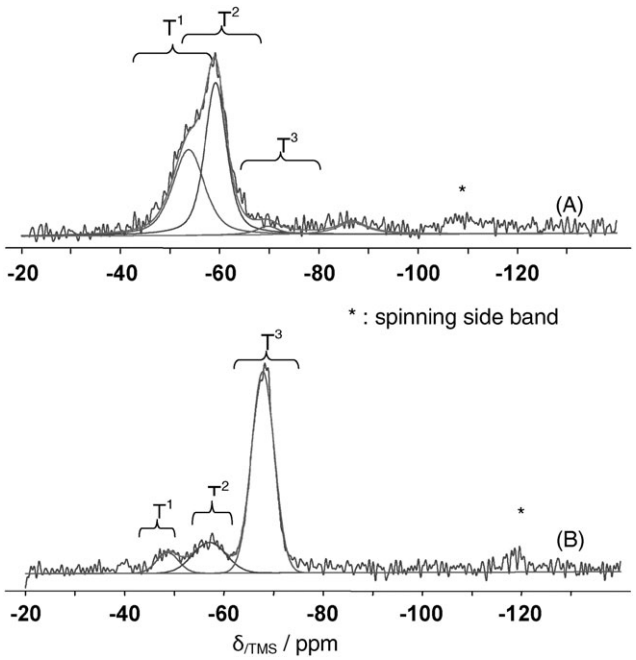

Fig. 8 ^{1}H decoupled ^{29}Si MAS NMR spectra of PAM-TLH (A) and PE-TLH (B) materials.

Table 4 ^{29}Si MAS NMR data (%) for PAM-TLH and PE-TLH materials

Sample	T^1	T^2	T^3
PAM-TLH	53	40	7
PE-TLH	8	18	74

Table 5 Chemical formulas, molar mass and organic content of PAM-TLH and PE-TLH samples deduced from chemical analysis and ^{29}Si MAS NMR results

Sample	Chemical formula	M/g mol^{-1}	Organic content (wt%)
PAM-TLH	$Na_{0.13}Mg_{2.98}(RSi)_{3.96}[O_{6.10}(OH)_{5.78}]$	802	51.5
PE-TLH	$Na_{0.18}Mg_{2.86}(RSi)_{4.03}[O_{8.32}OH)_{1.36}]$	766	55.2

of OH groups present in the tetrahedral sheets. The number of O atoms per half a unit cell can then be deduced assuming that the sum of the negative charges has to be equal to −18 according to the theoretical formula: $Mg_3(RSi)_4O_8(OH)_2$. Thus the second part of the chemical formulae of PAM-TLH and PE-TLH are $[O_{6.10}(OH)_{5.78}]$ and $[O_{8.32}(OH)_{1.36}]$, respectively.

The elemental analysis and ^{29}Si MAS NMR data allow the determination of the chemical formulae given in Table 5 and thus the molar weight per half a unit cell. Organic contents deduced from these results are in good agreement with both the theoretical and experimental values obtained by TG.

Conclusion

New lamellar organic–inorganic hybrids with a 2 : 1 talc-like structure have been synthesized. The X-ray diffraction

patterns as well as the elemental analysis suggest that these materials are close to the talc parent structure. The d_{001} periodicities extracted from the diffraction patterns are in favour of an alternated monolayer of straight phenylaminomethyl and bent phenethyl moieties. The ^{1}H-^{13}C CP MAS NMR magnetization curves, which are sensitive to mobility of the organic pendant groups, seem to indicate the lower mobility of phenylaminomethyl groups. Faults in the PAM-TLH structure revealed by ^{29}Si MAS NMR are probably induced by the rigidity of the phenylaminomethyl group and steric constraints. TEM micrographs gave insights in the morphology of the different materials. Well ordered stacking is observed for the phenylaminomethyl based material. The phenethyl based material reveals 25 nm length layers and a high tendency to exfoliate. This work drives to the conclusion that small differences on the alkoxysilane used for the sol–gel synthesis of lamellar organic–inorganic hybrids with a talc-like structure has strong consequences on the final material structure and properties. Studies on the preparation of nanocomposites based on these new materials are in progress.

Acknowledgements

The authors thank "La Fondation pour l'Ecole Nationale Supérieure de Chimie de Mulhouse" for the financial support, Wacker for the Geniosil XL 973 sample, Severinne Rigolet for NMR technical support, Jacques Baron for X-ray diffraction patterns, Laure Michelin for X-ray fluorescence analysis, Luc Delmotte for infrared spectrometry technical support and Loïc Vidal for TEM micrographs.

References

1 C. Sanchez, B. Julian, P. Belleville and M. Popall, *J. Mater. Chem.*, 2005, **15**, 3559–3592.
2 S. Williams-Daryn and R. K. Thomas, *J. Colloid Interface Sci.*, 2002, **255**, 303.
3 K. A. Carrado, L. Xu, R. Csencsits and J. V. Muntean, *Chem. Mater.*, 2001, **13**, 3766–3773.
4 Y. Fukushima and M. Tani, *J. Chem. Soc., Chem. Commun.*, 1995, 241–242.
5 L. Ukrainczyk, R. A. Bellman and A. B. Anderson, *J. Phys. Chem. B*, 1997, **101**, 531–539.
6 M. Jaber, J. Miehé-Brendlé, L. Delmotte and R. L. Dred, *Microporous Mesoporous Mater.*, 2003, **65**, 155–163.
7 M. Jaber, J. Miehé-Brendlé, L. Delmotte and R. Le Dred, *Solid State Sci.*, 2005, **7**, 610.
8 C. R. Silva, M. G. Fonseca, J. S. Barone and C. Airoldi, *Chem. Mater.*, 2002, **14**, 175–179.
9 J. A. A. Sales, G. C. Petrucelli, F. J. V. E. Oliveira and C. Airoldi, *J. Colloid Interface Sci.*, 2006, **297**, 95.
10 M. Richard-Plouet, S. Vilminot and M. Guillot, *New J. Chem.*, 2004, **28**, 1073–1082.
11 G. Kumaraswamy, Y. Deshmukh, V. V. Agrawal and P. Rajmohanan, *J. Phys. Chem. B*, 2005, **109**, 16034–16039.
12 M. G. Fonseca, C. R. Silva and C. Airoldi, *Langmuir*, 1999, **15**, 5048–5055.
13 M. G. Fonseca and C. Airoldi, *J. Chem. Soc., Dalton Trans.*, 1999, 3687–3692.
14 I. L. Lagadic, M. K. Mitchell and B. D. Payne, *Environ. Sci. Technol.*, 2001, **35**, 984–990.
15 B. Lebeau, N. T. Whilton and S. Mann, *Mater. Res. Soc. Symp. Proc.*, 2002, **726**, 27–32.
16 A. J. Patil, E. Muthusamy and S. Mann, *Angew. Chem., Int. Ed.*, 2004, **43**, 4928–4933.
17 I. L. Lagadic, *Microporous Mesoporous Mater.*, 2006, **95**, 226.
18 S. L. Burkett, A. Press and S. Mann, *Chem. Mater.*, 1997, **9**, 1071–1073.
19 M. Jaber, J. Miehé-Brendlé, L. Michelin and L. Delmotte, *Chem. Mater.*, 2005, **17**, 5275–5281.
20 D. Massiot, F. Fayon, M. Capron, I. King, S. L. Calvé, B. Alonso, J.-O. Durand, B. Bujoli, Z. Gan and G. Hoatson, *Magn. Reson. Chem.*, 2002, **1**, 70–76.
21 M. G. Fonseca, César R. Silva, José S. Barone and Claudio Airoldi, *Chem. Mater.*, 2002, **14**, 175–179.
22 M. Alexandre and P. Dubois, *Mater. Sci. Eng., R*, 2000, **28**, 1–63.
23 L.-Q. Wang, J. Liu, G. J. Exarhos, K. Y. Flanigan and R. Bordia, *J. Phys. Chem. B*, 2000, **104**, 2810–2816.
24 G. Engelhardt and D. Michel, *High-Resolution Solid-state NMR of Silicates and Zeolites*, John Wiley & Sons Ltd, Chichester, 1987.
25 S. R. Hartmann and E. L. Hahn, *Phys. Rev.*, 1962, 2042.

